ACS chemical biology

Letters

pubs.acs.org/acschemicalbiology

Impaired Transport of Nucleotides in a Mitochondrial Carrier Explains Severe Human Genetic Diseases

Stéphanie Ravaud,*[,†,‡,§,¶] Axel Bidon-Chanal,[∥,⊥,¶] Iulia Blesneac,[†,‡,§,#] Paul Machillot,[†,‡,§,□] Céline Juillan-Binard,[†,‡,§] François Dehez,*[,∥,⊥] Chris Chipot,*[,∥,⊥] and Eva Pebay-Peyroula*[,†,‡,§]

[†]Université Grenoble 1, IBS, Institut de Biologie Structurale, 41, rue Jules Horowitz, 38027 Grenoble cedex 1, France

[‡]CEA, IBS, Grenoble, France

[§]CNRS, IBS, Grenoble, France

[∥]Nancy Université, BP239, 54506 Vandoeuvre-lès-Nancy Cedex, France

[⊥]CNRS, SRSMC, Nancy, France

Supporting Information

ABSTRACT: The mitochondrial ADP/ATP carrier (AAC) is a prominent actor in the energetic regulation of the cell, importing ADP into the mitochondria and exporting ATP toward the cytoplasm. Severe genetic diseases have been ascribed to specific mutations in this membrane protein. How minute, well-localized modifications of the transporter impact the function of the mitochondria remains, however, largely unclear. Here, for the first time, the relationship between all documented pathological mutations of the AAC and its transport properties is established. Activity measurements combined synergistically with molecular-dynamics simulations demonstrate how all documented pathological mutations alter the binding affinity and the translocation kinetics of the nucleotides. Throwing a bridge between the pathologies and their molecular origins, these results reveal two distinct mechanisms responsible for AAC-related genetic disorders, wherein the mutations either modulate the association of the nucleotides to the carrier by modifying its electrostatic signature or reduce its conformational plasticity.

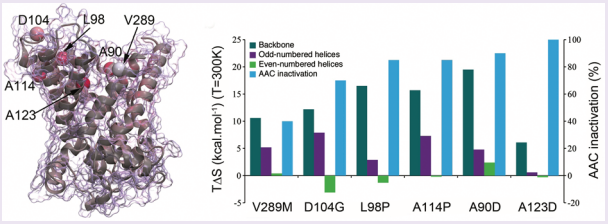

Mitochondrial carriers ensure the specific transport across the inner membrane of various metabolites required by key reactions occurring in mitochondria, such as oxidative phosphorylation, synthesis and degradation of amino acids and lipids, synthesis of iron−sulfur clusters and heme, as well as generation of heat by dissipation of the proton gradient (for a review, see ref 1). Impairing their function leads to severe diseases (*e.g.*, myopathies, congenital microcephaly, neonatal myoclonic epilepsy, HHH syndrome, hematological disorders) (see, for example, refs 2−4 and for a review, ref 5). The ADP/ATP carrier (AAC) is the best-known member of the mitochondrial carrier family (MCF).[6,7] Ubiquitous in the mitochondria of all eukaryotic cells, AAC specifically drives the import of ADP and the export of the newly synthesized ATP at the level of the inner membrane. Isoform 1 of the carrier (AAC1) is highly abundant in tissues where the energy demand is maximal and is specific to muscle and heart mitochondria where it represents up to 10% of the inner membrane proteins. Three main disorders associated with deficiencies of AAC1 have been described: AAC1 deficiency,[8] Sengers' syndrome,[9] and autosomal dominant progressive external ophthalmoplegia (adPEO).[10] Mutations of the AAC1 gene have been pinpointed for two of them: the recessive A123D mutation in patients affected with AAC1 deficiency, four heterozygous missense mutations (A90D, L98P, D104G, A114P) in adPEO families, and V289 M in a sporadic adPEO case. Several hypotheses have been put forth to explain the role of the mutations in these pathologies among which are (i) defective biogenesis of AAC1 in mitochondria, (ii) impairment of molecular interactions of AAC1 with key proteins, such as those forming the mitochondrial permeability transition pore, and (iii) dysfunction of the transport activity of AAC1, which could affect the mitochondrial pool of adenine nucleotides and cause mtDNA instability.[10−14] However, associated molecular mechanisms and structural basis remain largely unclear. None of these residues have been hitherto documented as key residues involved in substrate or inhibitor binding as deduced from the three-dimensional atomic structure[15] (Supplementary Figure S1).

The transport investigations conducted in a similar fashion for all six mutants, enabling their direct comparison, showed how the mutations altered the substrate affinity and/or the transport kinetics. MD simulations were carried out concomitantly to explore the structural and dynamic basis for the modification of these kinetic parameters. We report herein the first insights into the molecular details of how single-point

Received: January 9, 2012
Accepted: April 12, 2012
Published: April 12, 2012

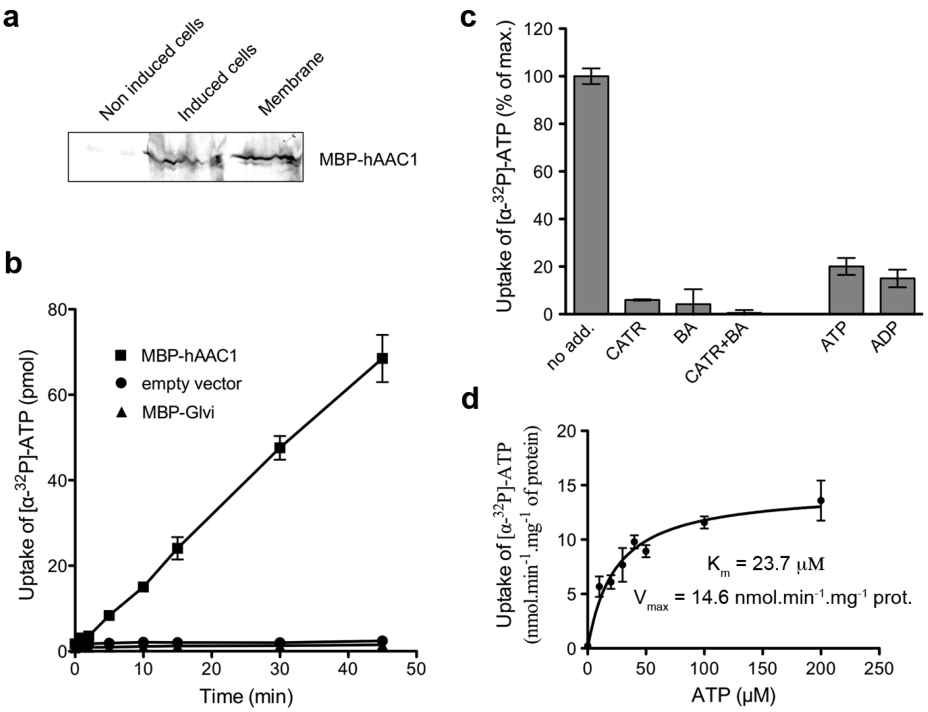

Figure 1. hAAC1 is functionally expressed in *E. coli* membranes. (a) Western blot analysis of the expression of MBP-hAAC1 in *E. coli* using an anti-MBP antibody. (b) Time dependency of [α-^{32}P]ATP uptake into cells expressing MBP-hAAC1 and the given controls incubated with 10 μM labeled ATP for the indicated time periods, as described in Methods. (c) [α-^{32}P]ATP uptake by *E. coli* expressing MBP-hAAC1 was measured in the presence of 10 μM labeled ATP and 100 μM inhibitors (CATR and/or BA) or of nonlabeled ADP or ATP. The rate of transport in the absence of additives was set to 100%. The control nucleotide uptake (empty vector) was subtracted. (d) Substrate saturation curve of [α-^{32}P]ATP uptake of cells expressing MBP-hAAC1. The control nucleotide uptake (empty vector) was subtracted. The K_m and V_{max} values were extrapolated from the experimental data fitted with the Michaelis–Menten equation. For all panels, data points and error bars are the mean ± SD of at least three independent experiments.

mutations can reduce the ATP level available in the cell by altering the transport from the mitochondrial matrix to the cytoplasm and, hence, be responsible for severe genetic diseases.

Functional Expression of hAAC1 in *E. coli*. Using the maltose-binding protein (MBP) as a fusion partner, we succeeded for the first time in expressing a functional human AAC1 (hAAC1) in the plasma membrane of *E. coli* (Figure 1a–c). The transport properties of hAAC1 were investigated directly in *E. coli* cells, which do not import ATP to fulfill its usual function. Cells expressing hAAC1 but not the control cells mediated uptake of [α-^{32}P]ATP above background levels (Figure 1b). The addition of the highly specific AAC inhibitors CATR (carboxyatractyloside) and BA (bongkrekic acid)[16,17] led to nearly complete inhibition (Figure 1c). The ATP import was substantially reduced by competition with excess ATP or ADP, the two exclusive substrates of AAC. The affinity for ADP being slightly higher than for ATP, ADP exhibited the strongest inhibition on ATP import affinity (Figure 1c). The dose–response curve indicates an apparent K_m for ATP of 23.7 ± 5 μM and a V_{max} of 14.6 ± 0.6 nmol min^{-1} mg^{-1} of protein (Figure 1d, Table 1). We have determined an apparent K_i of ADP on ATP uptake of 8.4 μM. Our results are comparable with the few data previously reported for hAAC1[11] and demonstrate that the main properties of the transporter are retained and can be assayed directly in *E. coli* cells (Figure 1).

Transport Properties of Pathological Mutants. The system described for the wild-type protein proves to be a powerful tool to study systematically the transport activity of all six pathological hAAC1 mutants (Figure 2, Table 1, Supplementary Figure S2). Uptake experiments revealed a decreased transport rate compared to the wild-type protein (Figure 2d). The mutations can be clustered into three groups depending on the degree of transport and ATP binding impairment: (i) V289M and D104G; (ii) L98P, A114P, and A90D; (iii) A123D. V289M and D104G only partially reduce transport. They retained approximately 60% and 30% of the wild-type activity, respectively. ATP binding is not affected, as seen from K_m values, whereas V_{max} values are, respectively, 1.5 and 3 times lower than that of the wild-type (Table 1). V289 and D104 are not strictly conserved among AACs, hence suggesting that their modification might not perturb nucleotide

Table 1. Kinetic Parameters of the Wild-Type Protein and of the Pathological Mutants[a]

	K_m (μM)	V_{max} (nmol ATP min^{-1} mg^{-1} of protein)
wild-type	23.7 ± 5	14.6 ± 0.6
A90D	82.1 ± 7.8	7.8 ± 0.4
L98P	18.5 ± 9.8	1.7 ± 0.3
D104G	15.9 ± 6.4	4.1 ± 0.4
A114P	104.1 ± 47.9	4.5 ± 1.1
A123D	ND[b]	ND[b]
V289M	17.0 ± 2.4	10.3 ± 0.4

[a] K_m and V_{max} values for ATP of the wild-type MBP-hAAC1 and of the 6 mutants heterologously expressed in *E. coli*. The values were computed from substrate saturation curves of [α-^{32}P]ATP uptake by cells expressing the different constructs (Supplementary Figure S2). Values are the mean ± SD of three independent experiments. [b] Not determined.

dx.doi.org/10.1021/cb300012j | *ACS Chem. Biol.* 2012, 7, 1164–1169

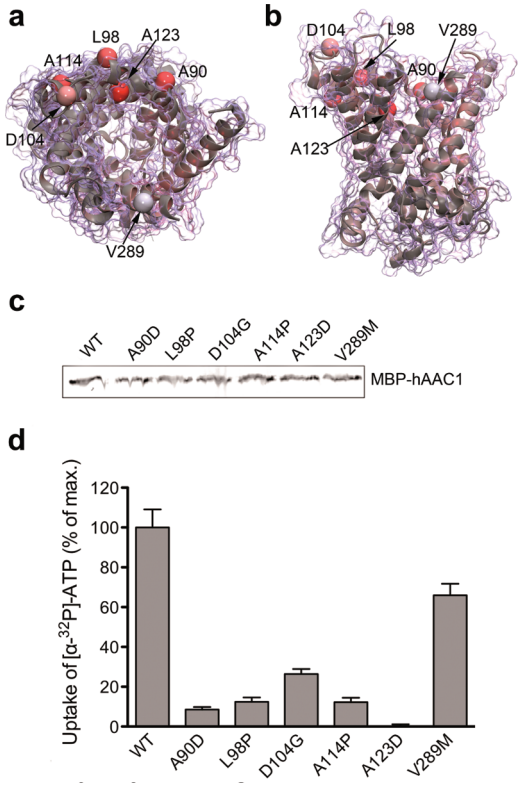

Figure 2. Transport properties of the pathological mutants. (a) Top and (b) side views of the AAC1 three-dimensional structure. A90 and L98 lie on the second half of H2, A114 and A123 are in the first half of H3, D104 is located in the C1 loop, and V289 is at the very end of H6. The residues are colored according to the impact of the mutations on the transport activity. (c) The 6 pathological mutants were expressed in *E. coli* as for the wild-type. The corresponding total cell extracts were analyzed by Western blot as in Figure 1a. (d) Transport activities of the mutants compared to the wild-type. The uptake of [α-^{32}P]ATP into intact *E. coli* cells expressing either the wild-type (WT) carrier or one of the 6 mutants was measured in the presence of 10 μM labeled ATP. Rates of [α-^{32}P]ATP uptake are given as a percentage of the rate of the wild-type protein.

binding, but only the transport efficiency. In line with our results, the symptomatology described for these two adPEO-associated mutants is one of the mildest, being limited to ptosis with a relatively late onset.[10,18] In contrast, the global activity of L98P, A114P, or A90D is strongly reduced to 10−15% in line with medical observations. Indeed, L98P is implicated in weakness, exercise intolerance, and bipolar affective disorder.[19] A114P is mainly associated with ophthalmoplegia.[10] A90D was identified in patients suffering from ptosis, exercise intolerance, and schizoaffective disorder.[20] Residues A90, L98, and A114 are all borne by helices H2 and H3 facing the funnel (Figure 2a, Supplementary Figure S1), but the transport properties of the corresponding mutants differ slightly. Only V_{max} is affected with L98P, whereas both K_m and V_{max} are modified for the others (Table 1). L98P is located at the very end of H2, which might explain the conserved K_m value. V_{max} is, however, dramatically reduced by a 10-fold decrease compared to the wild-type. It is worth noting that L98 is close to K92 and K96, two basic residues forming the upper basic patch that attracts nucleotides toward the cavity[21,22] (Figure 2a). Perturbing the environment of these residues is envisioned to modify the efficiency of nucleotide uptake. A90 and A114 are highly conserved among the AACs of all documented species and are found in highly conserved sequence stretches. Though they are not located at the bottom of the cavity that the nucleotide binds prior to transport (Figure 2a), ATP binding diminishes for both residues, as seen from the K_m values, 4 to 5 times lower than for the wild-type (Table 1). The mutations caused also a 2- to 3-fold decrease of V_{max}, respectively. Transport is totally abolished when A123, a highly conserved residue found deep in the cavity, is mutated into an aspartate (Figure 2a). A123D has been described in AAC1 deficiency , a disorder associated with severe myopathy and cardiomyopathy symptoms.[8]

Reconciling Transport Properties, Protein Flexibility, and Electrostatic Signature. All six mutations reported hitherto in relationship with human diseases are gathered near the intermembrane space and, barring D104G, interface with the membrane. All of them but one, namely, V289M, are clustered on the cytoplasmic halves of helices H2 and H3 (Figure 2a). In contrast, genetic variations observed among 1,000 presumably healthy humans highlight five single-point mutations in the protein sequence distributed within the structure (http://browser.1000genomes.org). In order to relate the degree of impairment and the changes in the transport efficacy to modifications in the structure, dynamics or electrostatic properties of the carrier, molecular-dynamics (MD) simulations have been performed on the wild-type carrier and the six mutants embedded in their lipid medium (Supplementary Figure S3). Neither a global nor a local structural reorganization was observed over the 100 ns time scale of the trajectories, except for A90D. The carboxylic moiety of D90 switches its orientation from the interior of the membrane to the aqueous medium, resulting ultimately in a local distortion of H2 (Supplementary Figure S4), in line with modified accessibilities observed from cysteine scans.[23]

Although the entire mechanism that underlies the conformational transformations enabling transport has not been yet deciphered, a number of studies have hinted at the crucial role of the flexibility of AAC to interconvert.[6] Simulations of the A114P pathological mutant and its revertant, A114P/V181M, recently suggested that the dynamics of the protein is modified with the former mutation and is restored with the latter.[24] Protein flexibility is known to be pivotal in many biological processes embracing among others protein−protein and protein−ligand recognition and association, as well as protein folding and allosteric regulation. Correlation between this property and nucleotide transport was investigated by means of *B*-factors, together with configurational entropies inferred from atomic positional fluctuations computed along each trajectory (Figure 3a). Zero-mean symmetrical distributions reflect similarity in the overall flexibility of the two proteins, as can be seen for mutants A123D, D104G, and V289M. In contrast, skewed distributions, offset toward positive values of the difference in *B*-factors betoken an altogether rigidified carrier in A90D, A114P and L98P. These results suggest that loss of flexibility and transport are intimately related. Backbone configurational entropies have been estimated in the pseudoharmonic approximation[25] (Figure 3b). Except for A123D, the hierarchy of entropy loss correlates nicely with the experimentally observed alteration of nucleotide-transport activity in AAC single mutants. Detailed analysis further reveals that even-numbered helices (Figure 3b) are marginally affected. In sharp contrast, plasticity of odd-numbered helices is markedly diminished compared to that of the wild-type AAC, congruent with previous observations.[6]

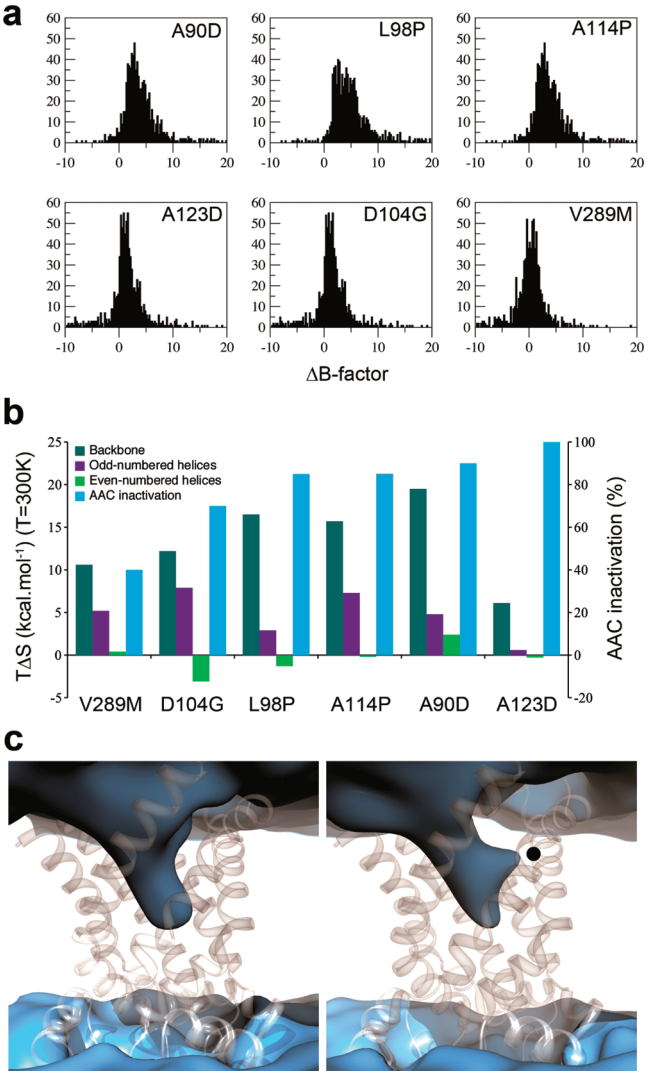

Figure 3. Nucleotide transport is correlated to protein flexibility or to electrostatic signature. (a) Distribution of the differences in *B*-factors computed over the backbone atoms of the WT protein with respect to the mutants. The Δ*B*-factor ($B_{WT} - B_{mutant}$) is given in Å^2. (b) Differences in configurational entropies for each mutant $T(S_{WT} - S_{mutant})$ on the left compared to the inactivation percentile with respect to the WT carrier on the right. The values are shown for the protein backbone, as well as for the odd- and even-numbered helices separately, according to the color code indicated on the figure. (c) Three-dimensional electrostatic potential maps for the WT *apo* protein (left) and for the A123D *apo* mutant (right). The position of the point mutation is highlighted with a black sphere. Both isopotential surfaces correspond to the same electrostatic potential value of −12 kT/e and were obtained with the PMEPot[33] module of VMD[34] using a grid-spacing of <1 Å and an ewald factor of 0.25.

Another feature crucial for transport is the electrostatic signature of the carrier.[21,26] In the conformation of AAC open toward the intermembrane space, this signature consists of a funnel that drives ADP^{3-} to the bottom of the internal cavity. Replacement by aspartate of the neutral side chain of A123 markedly reshapes the topology of the local electric field (Figure 3c), at variance with the other mutations (Supplementary Figure S5). No other structural or dynamical difference was recorded. Such an alteration of the electrostatic fingerprint of the carrier is anticipated to hamper significantly binding of ADP^{3-} or ATP^{4-}, consistent with the inactivation measured experimentally. In addition, MD simulations revealed that ADP is not attracted into the cavity of the A123D mutant (Supplementary Figure S6). The strongly reduced transport activity can, therefore, be ascribed to the difficulty for ADP to reach its dedicated binding site at the bottom of the cavity, a scenario akin to the inhibitory effect of high chloride concentrations.[27]

Our experimental model gives access to direct measurements of transport properties of hAAC1, unlike previous studies performed in yeast. Altogether, our results on hAAC1 suggest two molecular mechanisms whereby mutations can modulate and possibly obliterate AAC activity. First, reduction of the overall flexibility of the protein is likely to thwart the conformational change that accompanies nucleotide binding and/or transport affecting K_m and/or V_{max}. AAC is one of the first examples wherein mutations distant from the nucleotide-binding site modify the functional properties of the protein by reducing its flexibility. Second, alteration of the topology of the electrostatic funnel is expected to hobble binding of ADP^{3-} to the carrier. The six mutants implicated in genetic diseases obey one of the above mechanisms. The methodology followed herein illuminates the possible molecular mechanisms that underlie severe diseases, while paving the way to address the deleterious effects of other mutations and explore novel, well-adapted therapeutic strategies.

METHODS

Transport Activity Measurements in *E. coli* Cells. The MBP-hAAC1 construct encodes an in frame fusion of a periplasmic MBP at the N-terminus of hAAC1. The hAAC1 point mutations were introduced in the MBP-hAAC1 construct by site directed mutagenesis. The uptake of [α-^{32}P]-labeled ATP was determined for intact *E. coli* C43 (DE3) cells expressing MBP-hAAC1, the MBP-hAAC1 mutants, or the given controls. Dose−response curves and experiments used to investigate substrate specificity and effects of the inhibitors were carried out by modified published methods.[28,29]

MD Simulations. The initial AAC structure was obtained as previously described,[21,27] and the mutants were generated from an equilibrated structure of the wild-type protein. All simulations were performed in the isothermal−isobaric ensemble with the protein inmersed in a fully hydrated palmitoyl-oleyl-phosphatidyl-choline (POPC) bilayer. The system was simulated using the all-atom CHARMM27[30,31] force field for the protein, waters, and ions and the modified united-atom version for the lipids;[32] 100-ns trajectories were produced for each system, from which only the last 30 ns were used for analysis. For the backbone atoms (CA, N, C, and O), *B*-factors were inferred from the atomic positional fluctuations. Configurational entropies were computed using the pseudoharmonic approach of Schlitter.[25]

ASSOCIATED CONTENT

Supporting Information

Additional figures and detailed methods. This material is available free of charge *via* the Internet at http://pubs.acs.org.

AUTHOR INFORMATION

Corresponding Author

*E-mails: stephanie.ravaud@ibs.fr; Francois.Dehez@edam.uhp-nancy.fr; Christophe.Chipot@edam.uhp-nancy.fr; eva.pebay-peyroula@ibs.fr.

Present Addresses

#IGF, CNRS/INSERM/Universités Montpellier, 34094 Montpellier, France.

□DSV/iBITec-S, CEA Saclay, 91191 Gif sur Yvette Cedex, France.

Author Contributions

¶These authors contributed equally to this work.

Notes

The authors declare no competing financial interest.

■ ACKNOWLEDGMENTS

We thank A. Frelet-Barrand for her help in the uptake experiments, E. M. Krammer for the initial MD setup, and N. Cherradi and O. Filhol-Cochet for access to the radioactivity room (CEA/iRTSV). The work was supported by the Institut Universitaire de France, by ANR (Trans-MIT, MIT-2M), and by E.U. project EDICT nr 211800. The Grand Equipement National de Calcul Informatique and Centre Informatique National de l'Enseignement Supérieur are gratefully acknowledged for provision of computer time.

■ REFERENCES

(1) Kunji, E. R. (2004) The role and structure of mitochondrial carriers. *FEBS Lett. 564*, 239−244.

(2) Graham, B. H., Waymire, K. G., Cottrell, B., Trounce, I. A., MacGregor, G. R., and Wallace, D. C. (1997) A mouse model for mitochondrial myopathy and cardiomyopathy resulting from a deficiency in the heart/muscle isoform of the adenine nucleotide translocator. *Nat. Genet. 16*, 226−234.

(3) Wallace, D. C. (1999) Mitochondrial diseases in man and mouse. *Science 283*, 1482−1488.

(4) Guernsey, D. L., Jiang, H., Campagna, D. R., Evans, S. C., Ferguson, M., Kellogg, M. D., Lachance, M., Matsuoka, M., Nightingale, M., Rideout, A., Saint-Amant, L., Schmidt, P. J., Orr, A., Bottomley, S. S., Fleming, M. D., Ludman, M., Dyack, S., Fernandez, C. V., and Samuels, M. E. (2009) Mutations in mitochondrial carrier family gene SLC25A38 cause nonsyndromic autosomal recessive congenital sideroblastic anemia. *Nat. Genet. 41*, 651−653.

(5) Palmieri, F. (2008) Diseases caused by defects of mitochondrial carriers: a review. *Biochim. Biophys. Acta 1777*, 564−578.

(6) Nury, H., Dahout-Gonzalez, C., Trezeguet, V., Lauquin, G. J., Brandolin, G., and Pebay-Peyroula, E. (2006) Relations between structure and function of the mitochondrial ADP/ATP carrier. *Annu. Rev. Biochem. 75*, 713−741.

(7) Klingenberg, M. (2008) The ADP and ATP transport in mitochondria and its carrier. *Biochim. Biophys. Acta 1778*, 1978−2021.

(8) Palmieri, L., Alberio, S., Pisano, I., Lodi, T., Meznaric-Petrusa, M., Zidar, J., Santoro, A., Scarcia, P., Fontanesi, F., Lamantea, E., Ferrero, I., and Zeviani, M. (2005) Complete loss-of-function of the heart/muscle-specific adenine nucleotide translocator is associated with mitochondrial myopathy and cardiomyopathy. *Hum. Mol. Genet. 14*, 3079−3088.

(9) Jordens, E. Z., Palmieri, L., Huizing, M., van den Heuvel, L. P., Sengers, R. C., Dorner, A., Ruitenbeek, W., Trijbels, F. J., Valsson, J., Sigfusson, G., Palmieri, F., and Smeitink, J. A. (2002) Adenine nucleotide translocator 1 deficiency associated with Sengers syndrome. *Ann. Neurol. 52*, 95−99.

(10) Kaukonen, J., Juselius, J. K., Tiranti, V., Kyttala, A., Zeviani, M., Comi, G. P., Keranen, S., Peltonen, L., and Suomalainen, A. (2000) Role of adenine nucleotide translocator 1 in mtDNA maintenance. *Science 289*, 782−785.

(11) De Marcos Lousa, C., Trezeguet, V., Dianoux, A. C., Brandolin, G., and Lauquin, G. J. (2002) The human mitochondrial ADP/ATP carriers: kinetic properties and biogenesis of wild-type and mutant proteins in the yeast *S. cerevisiae*. *Biochemistry 41*, 14412−14420.

(12) Fontanesi, F., Palmieri, L., Scarcia, P., Lodi, T., Donnini, C., Limongelli, A., Tiranti, V., Zeviani, M., Ferrero, I., and Viola, A. M. (2004) Mutations in AAC2, equivalent to human adPEO-associated ANT1 mutations, lead to defective oxidative phosphorylation in *Saccharomyces cerevisiae* and affect mitochondrial DNA stability. *Hum. Mol. Genet. 13*, 923−934.

(13) Thomas, A., Rey, M., Aubry, L., and Pelosi, L. (2011) A hybrid model to study pathological mutations of the human ADP/ATP carriers. *Biochimie 93*, 1415−1423.

(14) Kawamata, H., Tiranti, V., Magrane, J., Chinopoulos, C., and Manfredi, G. (2011) adPEO mutations in ANT1 impair ADP-ATP translocation in muscle mitochondria. *Hum. Mol. Genet. 20*, 2964−2974.

(15) Pebay-Peyroula, E., Dahout-Gonzalez, C., Kahn, R., Trezeguet, V., Lauquin, G. J., and Brandolin, G. (2003) Structure of mitochondrial ADP/ATP carrier in complex with carboxyatractyloside. *Nature 426*, 39−44.

(16) Vignais, P. V., Vignais, P. M., and Stanislas, E. (1962) Action of potassium atractylate on oxidative phosphorylation in mitochondria and in submitochondrial particles. *Biochim. Biophys. Acta 60*, 284−300.

(17) Henderson, P. J., and Lardy, H. A. (1970) Bongkrekic acid. An inhibitor of the adenine nucleotide translocase of mitochondria. *J. Biol. Chem. 245*, 1319−1326.

(18) Komaki, H., Fukazawa, T., Houzen, H., Yoshida, K., Nonaka, I., and Goto, Y. (2002) A novel D104G mutation in the adenine nucleotide translocator 1 gene in autosomal dominant progressive external ophthalmoplegia patients with mitochondrial DNA with multiple deletions. *Ann. Neurol. 51*, 645−648.

(19) Siciliano, G., Tessa, A., Petrini, S., Mancuso, M., Bruno, C., Grieco, G. S., Malandrini, A., DeFlorio, L., Martini, B., Federico, A., Nappi, G., Santorelli, F. M., and Murri, L. (2003) Autosomal dominant external ophthalmoplegia and bipolar affective disorder associated with a mutation in the ANT1 gene. *Neuromuscular Disord. 13*, 162−165.

(20) Deschauer, M., Hudson, G., Muller, T., Taylor, R. W., Chinnery, P. F., and Zierz, S. (2005) A novel ANT1 gene mutation with probable germline mosaicism in autosomal dominant progressive external ophthalmoplegia. *Neuromuscular Disord. 15*, 311−315.

(21) Dehez, F., Pebay-Peyroula, E., and Chipot, C. (2008) Binding of ADP in the mitochondrial ADP/ATP carrier is driven by an electrostatic funnel. *J. Am. Chem. Soc. 130*, 12725−12733.

(22) Pebay-Peyroula, E., and Brandolin, G. (2004) Nucleotide exchange in mitochondria: insight at a molecular level. *Curr. Opin. Struct. Biol. 14*, 420−425.

(23) Kihira, Y., Iwahashi, A., Majima, E., Terada, H., and Shinohara, Y. (2004) Twisting of the second transmembrane alpha-helix of the mitochondrial ADP/ATP carrier during the transition between two carrier conformational states. *Biochemistry 43*, 15204−15209.

(24) Di Marino, D., Oteri, F., Morozzo Della Rocca, B., Chillemi, G., and Falconi, M. (2010) ADP/ATP mitochondrial carrier MD simulations to shed light on the structural-dynamical events that, after an additional mutation, restore the function in a pathological single mutant. *J. Struct. Biol. 172*, 225−232.

(25) Schlitter, J. (1993) Estimation of absolute and relative entropies of mac- romolecules using the covariance matrix. *Chem. Phys. Lett. 215*, 617−621.

(26) Wang, Y., and Tajkhorshid, E. (2008) Electrostatic funneling of substrate in mitochondrial inner membrane carriers. *Proc. Natl Acad. Sci. U.S.A 105*, 9598−9603.

(27) Krammer, E. M., Ravaud, S., Dehez, F., Frelet-Barrand, A., Pebay-Peyroula, E., and Chipot, C. (2009) High-chloride concentrations abolish the binding of adenine nucleotides in the mitochondrial ADP/ATP carrier family. *Biophys. J. 97*, L25−27.

(28) Haferkamp, I., Hackstein, J. H., Voncken, F. G., Schmit, G., and Tjaden, J. (2002) Functional integration of mitochondrial and hydrogenosomal ADP/ATP carriers in the Escherichia coli membrane reveals different biochemical characteristics for plants, mammals and anaerobic chytrids. *Eur. J. Biochem. 269*, 3172−3181.

(29) Tsaousis, A. D., Kunji, E. R., Goldberg, A. V., Lucocq, J. M., Hirt, R. P., and Embley, T. M. (2008) A novel route for ATP acquisition by the remnant mitochondria of *Encephalitozoon cuniculi*. *Nature 453*, 553−556.

(30) Mackerell, A. D., Jr., Bashford, D., Bellott, M., Dunbrack, R. L., Evanseck, J. D., Field, M. J., Fischer, S., Goa, J., Guo, H., Ha, S.,

Joseph-McCarthy, D., Kuchnir, L., Lau, F. T. K., Mattos, C., Mich-Nick, S., Ngo, T., Nguyen, D. T., Prodhom, B., Reiher, W. E., Roux, B., Schlenkrich, M., Smith, J. C., Stote, R., Straub, J., Watanabe, M., Wiorkiewicz-Kuczera, J., Yin, D., and Karplus, M. (1998) All-atom empirical potential for molecular modeling and dynamics studies of proteins. *J. Phys. Chem. B102*, 3586−3616.

(31) Feller, S. E., and Mackerell, A. D., Jr. (2000) All-atom empirical force field for nucleic acids: I. Parameter optimization based on small molecule and condensed phase macromolecular target data. *J. Phys. Chem. B104*, 7510−7515.

(32) Henin, J., Shinoda, W., and Klein, M. L. (2008) United-atom acyl chains for CHARMM phospholipids. *J. Phys. Chem. B 112*, 7008−7015.

(33) Aksimentiev, A., and Schulten, K. (2005) Imaging alpha-hemolysin with molecular dynamics: ionic conductance, osmotic permeability, and the electrostatic potential map. *Biophys. J. 88*, 3745−3761.

(34) Humphrey, W., Dalke, A., and Schulten, K. (1996) VMD - Visual Molecular Dynamics. *J. Mol. Graphics 97*, 25−27.